

HEAT SINK PERFORMANCE AND THERMAL ANALYSIS USING CFD WITH VARIOUS FIN CONFIGURATIONS

RUSHIKESH DHAS

Heat and Power Engineering, Mechanical Engineering Department, Vishwakarma Institute of Technology, Pune.
Email: rushikesh.dhas19vit.edu

L. D. MANGATE

Coordinator of Heat and Power Engineering, Mechanical Engineering Department, Vishwakarma Institute of Technology, Pune.

Abstract

The optimum Heat Sink for effective cooling of electrical gadgets is what this paper aims to demonstrate. As heat sinks are frequently utilized in electronic components to enhance heat transfer, this work compares a heat sink with fins of various profiles, including square, circular, triangular, and hexagonal fins. This study proposes a novel approach for cooling electronic components through the use of heat sinks composed of aluminum alloy. Several geometric factors need to be taken into account, such as the length and thickness of fins, the quantity of fins, the thickness of the base plate, the spacing between fins, the shape or profile of the fins, and the material used, among others, the selection of the optimal heat sink is influenced by multiple geometric factors. Therefore, to address this, initial investigations have been performed using computational fluid dynamics (CFD) simulations to analyze the fluid flow and heat transfer traits of different conventional steady heat sink designs. In order to determine how different fin arrays' geometrical fin characteristics affect natural convection heat transfer, CFD analysis is used. Ansys Workbench 19.0, which was used in our investigation, was used to build Computational Fluid Dynamics. A finite-volume control volume-based approach used to solve governing equations. Utilizing computational fluid dynamics, the momentum equations' velocity and pressure components are interdependent and cannot be analyzed independently of each other. Heat transfer using aluminum 6061 as a pin fin material and ambient air. For the purpose of analyzing the thermal efficiency of various pin fins, measuring their thermal resistance, pressure drop, heat transfer coefficients, as well as predicting the smallest temperature variation across the fins for the various fin profiles' heat sinks at diverse velocities and a constant heat supply of 15W, the inlet air temperature of 295 K is used. This study's objective is to investigate the impact of various pin-fin arrangements. The results demonstrate that the Elliptical fin of hydraulic diameter 4.51 mm diameter with 3.38 mm fin spacing and heat sink demonstrates improved performance at a velocity of 12 m/s because the minimum thermal resistance and maximum heat transfer coefficient. In comparison to other scenarios and fin heat sink types, the thermal resistance of this particular configuration measures 2.977K, while the heat transfer coefficient is 335 W/m²K. Moreover, the pressure drop is 61 Pa lower than the other cases.

Keywords: Heat Sink, Computational Fluid Dynamics, Natural convection, Surface Nusselt number, Pressure drop, Thermal resistance, Heat transfer coefficient

INTRODUCTION

In several industries electronic and, mechanical industry heatsinks are used for heat dissipation from hot surfaces or heat-generating bodies and reduce temperature up to ambient like air or water, in this work we are considering air as the surrounding medium.

By using a heat sink we can increase surface area for increased heat transfer coefficient as well. The key function of heat sink is to bring down the temperature to a level that falls within the allowable limits.

In recent years, there has been a significant increase in the generation of heat in microelectronic devices. Such devices commonly encounter thermal failures, which are a defect related to heating. Effective removal of heat energy is crucial for the proper functioning of electronic equipment, such as laptops, as overheating has been known to cause device failure. Laptop computers are one example of gadgets where heat management could potentially become an issue. High-speed computer makers recently had to recall certain equipment because of temperature-related issues. By increasing heat dissipation from the device, a heat sinking device may be utilized to minimize thermally triggered failures. A heat sink is a structural device that removes heat from an electronic circuit so that it can operate within acceptable temperature ranges.

Application of heat sink

Heat sinks are now widely available and used in various industries worldwide, including electronic cooling, audio, industrial control, defense, and telecommunications.

In many industrial applications, heat sinks are commonly utilized to cool electrical, power electronic, automotive, and telecommunications components. These parts could be integrated circuits like audio amplifiers, microcontrollers, microprocessors, or high-power semiconductor devices like diodes and thyristors. To be more accurate, quiescent cooling heat sinks are commonly used for cooling CPUs and audio amplifiers.

Objectives

- To design heat sink for given fin height and given base heat supply.
- In this work we analyze heat sink with different fin cross-sections like square, triangular, ellipse, and circular for different inlet velocities and the same hydraulic diameter.
- To predict the optimum shape of the fin heat input at the base is 9 KW

Building of Cad model

In this research work, we design a heat sink having shapes of fins are square, ellipse, circular, and triangular in the inline arrangement. By using design modular 101.43mm* 101.43mm* 5mm base plate created and used commonly for all heat sink designs. In heat sink, design fin spacing and fin height are kept constant. As we keep hydraulic diameter constant, it can change the number of fins.

Table 1.1: Selection of material

Properties	Aluminum	Air
Thermal conductivity(K)	202.4(w/mk)	0.026(w/mk)
Specific heat (Cp)	871(J/KgK)	1006.43(J/KgK)
Density	2719 (kg/m ³)	1.1965(kg/m ³)

Selection of material for heat

Architectural alloy al 6061 is the popular name for the medium strength aluminum alloy. It typically finds use in complex extrusions. It is easy to anodize, has a high level of corrosion resistance, and has a nice surface finish. Make sure the extrudability is good

CFD Modelling

Using numerical analysis and algorithms, the field of computational fluid dynamics (CFD) solves and studies issues involving fluid flows.

The following lists the assumptions that were made to make it easier to solve the models.

- 1) At film temperature, air properties are measured.
- 2) Laminar and constant airflow is present.
- 3) The fin itself does not generate any internal heat..
- 4) The heat transfer caused by radiation is minimal.
- 5) The fin's base experiences a constant temperature.

As time passes, the temperature and heat flow within the fin remains constant.

Boundary Conditions

The blocks are modeled in this analysis, except the heat sink, which is treated as a solid domain with a 9KW heat source. Aluminum 6061 is the heat sink material in this instance. At 300K, the analysis is conducted in the atmosphere.

The specified boundary conditions have been inputted/entered.:

- Base plate: - A 9 KW heat load and the characteristics of the alloy aluminum are given.
- Base top(wall): The base top receives heat from the chip, causing heat flux to be applied to the base top.
- Fin bottom, Front face, Left, Right, Rear face (Walls): Heat transmission to surrounds
- atmosphere through convection. air penetrates the heat sink at speeds of 4, 8, and 12 m/s, respectively.
- Outlet (Pressure Outlet): At the outlet, atmospheric pressure is assumed when air enters the atmosphere after passing through the heat sink.
- Following the application of the aforementioned boundary conditions. Up to convergence, simulation is run in a steady state.

Governing Equations

The laws of conservation of mass, momentum, and energy constitute foundation for heat transfer. All of the P-V-T (thermodynamics) properties are taken to be constant. The following is a textual representation of the continuity, momentum, and energy equation. The equation of state and the x-y and z-direction, momentum, and energy equations of Navier-Stokes's equations.

NOMENCLATURE

L=Fin height (mm)
 w = Fin Width (mm)
 S = fin Spacing (mm)
 U = Air inlet velocity (m/s)
 Cp = Specific Heat (J/kgK)
 ΔP = pressure drop along heat sink (Pa)
 h = Heat transfer coefficient (W/m^2K)
 K= Thermalconductivity (W/mK)
 Q = Heat Load (W)
 T = Temperature, (K)
 R = Thermal Resistance, (K/W)
 V = Volume (m^3)
 A= Surface Area (m^2)
 μ = dynamic viscosity (kg/ms)
 ν = kinematic viscosity (m^2/s)
 ρ = fluid density (kg/m^3)
 P=Pressure (Pa)
 Nu= Nusselt Number

Mesh Generation

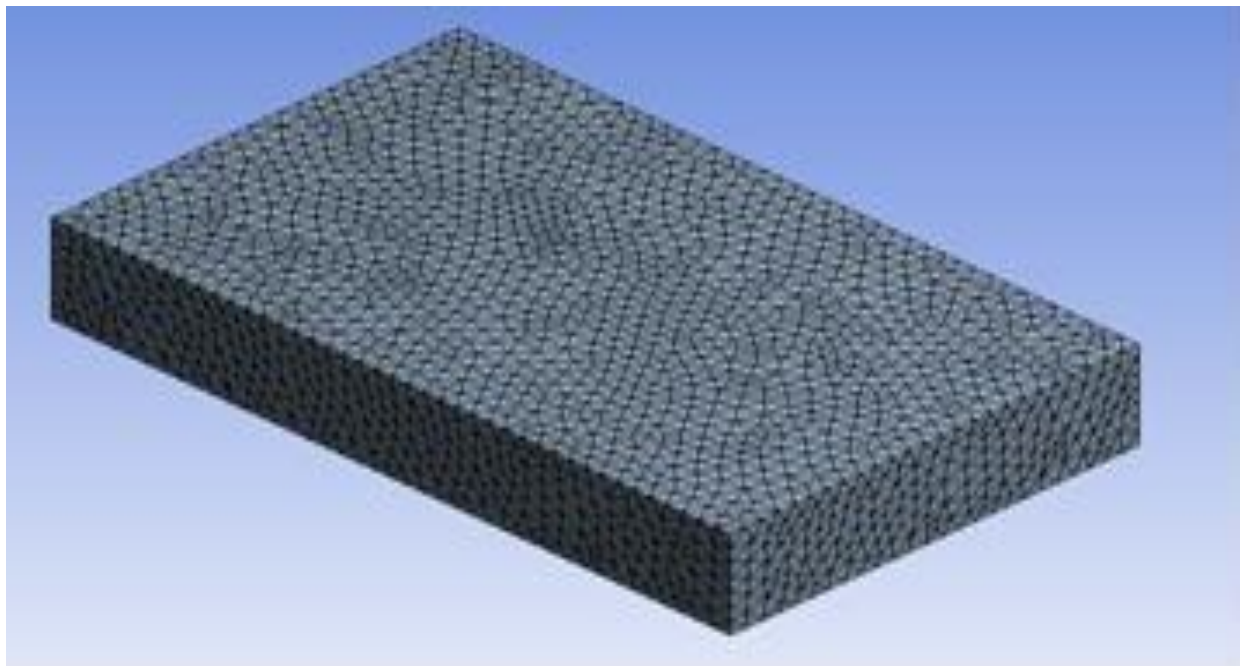


Fig 1.01: Meshing of the Fluid Enclosure

Mesh generation is the second step in pre-processing. The mesh creation process is started once the model has been imported into Ansys Workbench. There are several mesh sizes, including coarse, medium, and fine. A high-quality solution's essential element is mesh. Tetrahedral CFD meshes is used for our issue.



Fig 1.02: Meshing a Heat Sink Having Hexagonal Fins

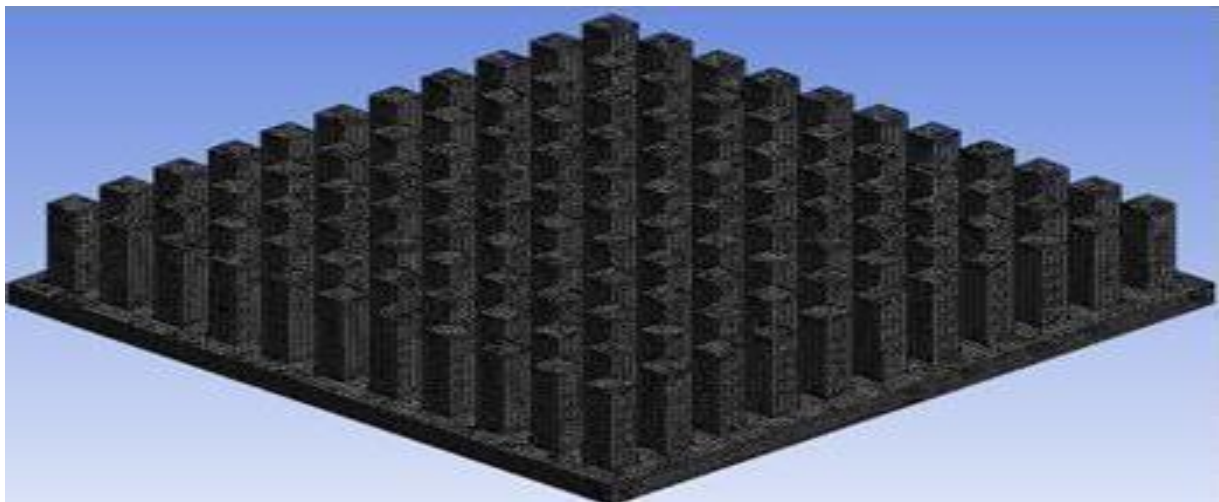


Fig 1.03: Meshing a Heat Sink Having Square Fins

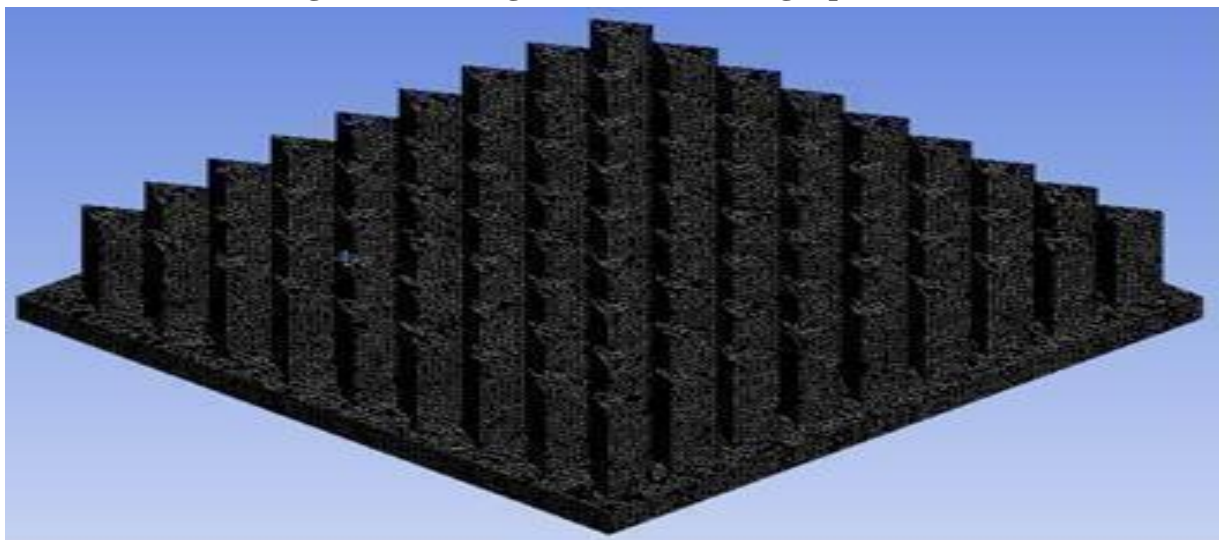


Fig 1.04: meshing a heat sink having elliptical fins

Process of solving governing equations is carried out using CFD

Law of Conservation of Mass

$$\frac{\partial \rho}{\partial t} + \nabla \cdot (\rho V) = 0 \quad (1)$$

Momentum Equation

X- Momentum

$$\frac{\partial(\rho u)}{\partial t} + \nabla \cdot (\rho u V) = -\frac{\partial \rho}{\partial x} + \frac{\partial c_{xx}}{\partial x} + \frac{\partial c_{yx}}{\partial y} + \frac{\partial c_{zx}}{\partial z} + S_{Mx} \quad (2)$$

Y-Momentum

$$\frac{\partial(\rho u)}{\partial t} + \nabla \cdot (\rho u V) = -\frac{\partial \rho}{\partial t} + \frac{\partial c_{xy}}{\partial x} + \frac{\partial c_{yy}}{\partial y} + \frac{\partial c_{zy}}{\partial z} + S_{My} \quad (3)$$

Z-Momentum

$$\frac{\partial(\rho w)}{\partial t} + \nabla \cdot (wV) = -\frac{\partial \rho}{\partial z} + \frac{\partial c_{xz}}{\partial x} + \frac{\partial c_{zy}}{\partial y} + \frac{\partial c_{zz}}{\partial z} + S_{Mz} \quad (4)$$

Energy Equation

$$\frac{\partial(\rho h_0)}{\partial t} + \nabla \cdot (\rho h_0 V) = -\rho \nabla \cdot V + \nabla \cdot (k \nabla T) + \varphi + S_h \quad (5)$$

Equation of State

$$\rho RT \quad (6)$$

Thermal Analysis Methodology

Rth=ΔT is the formula for calculating the heat sink's thermal resistance, Rth

Q

Through CFD simulations, the temperature difference is estimated.

T is calculated as the temperature differential between the greatest temperature at fin base and the surrounding air, and Q is the heat dissipation power applied in

Where,

Q =the amount of heat that is transported per unit of time (W)

A =the surface's area used for heat transfer (m²)

hc = coefficient of convective heat transfer for the given procedure (W/m²K).

ΔT = difference between temperature surface and bulk fluid (in K or °C)

RESULT AND DISCUSSIONS

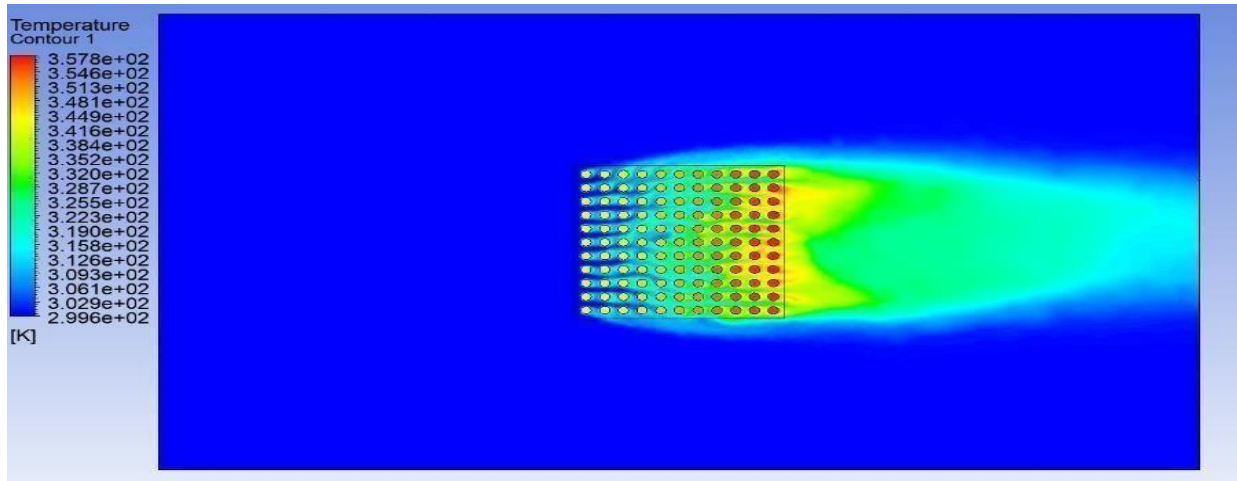


Fig 1.05: contour illustrates the lowest temperature distribution of a circular heat sink while it moves at a velocity of 4 m/s

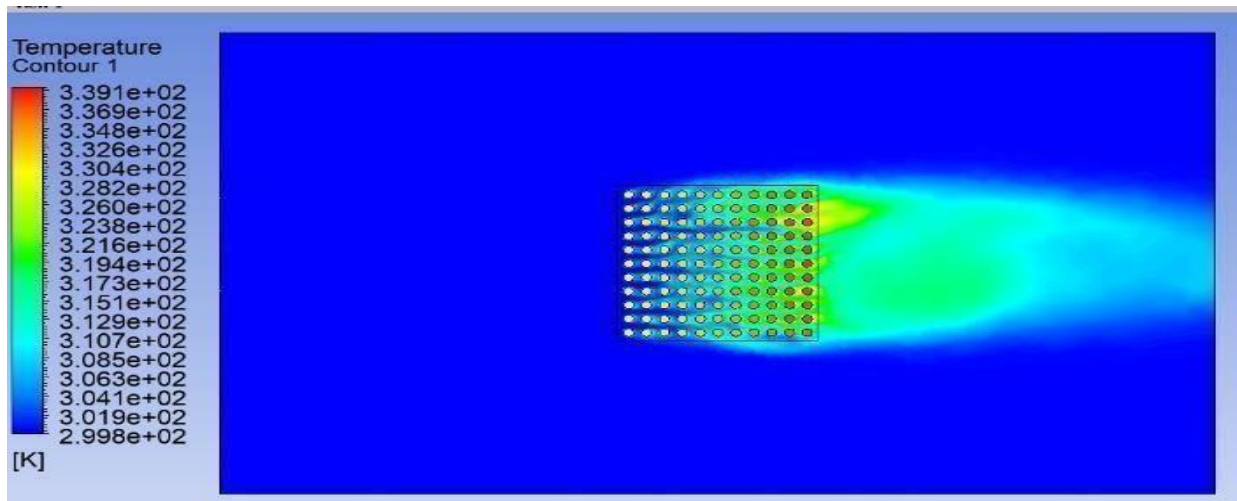


Fig 1.06: contour illustrates the lowest temperature distribution of a circular fin heat sink while it moves at a velocity of 8 m/s

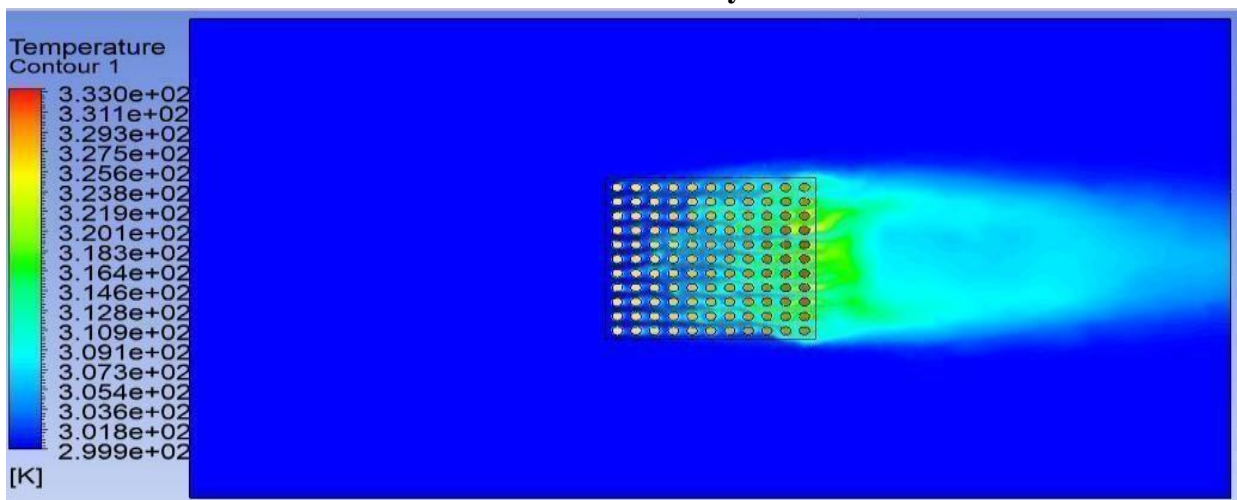


Fig 1.07: contour illustrates the lowest temperature distribution of a circular fin heat sink while it moves at a velocity of 12 m/s

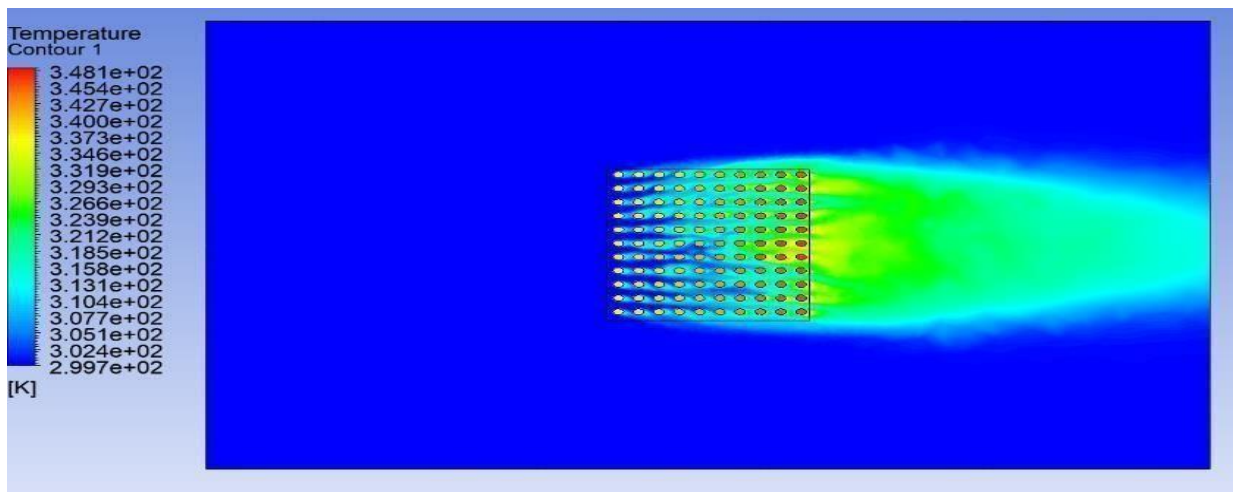


Fig 1.08: contour illustrates the lowest temperature distribution of an ellipse fin heat sink while it moves at a velocity of 4 m/s

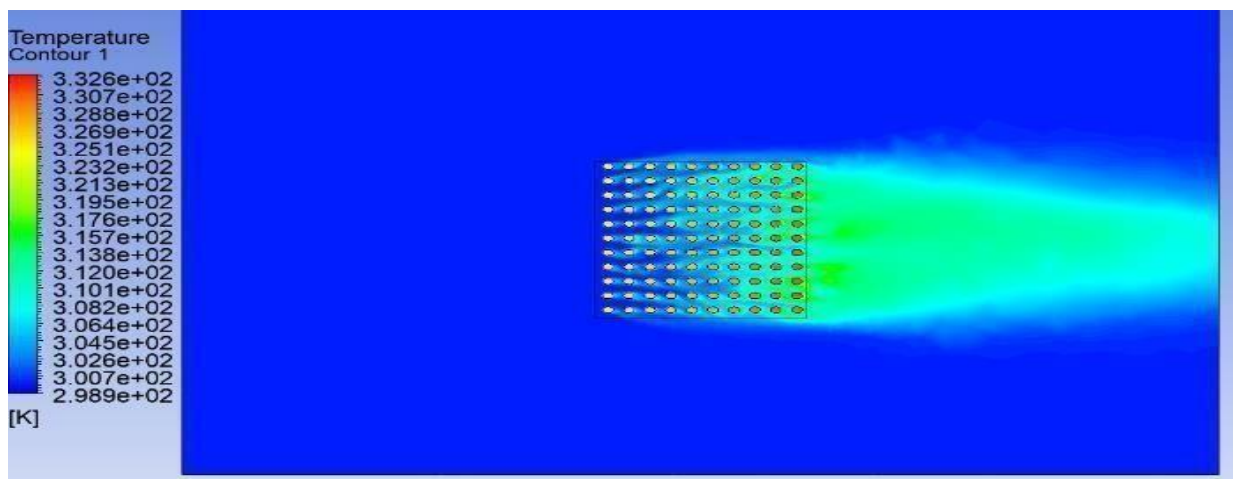


Fig 1.09: contour illustrates the lowest temperature distribution of an ellipse fin heat sink while moves at velocity 8m/s

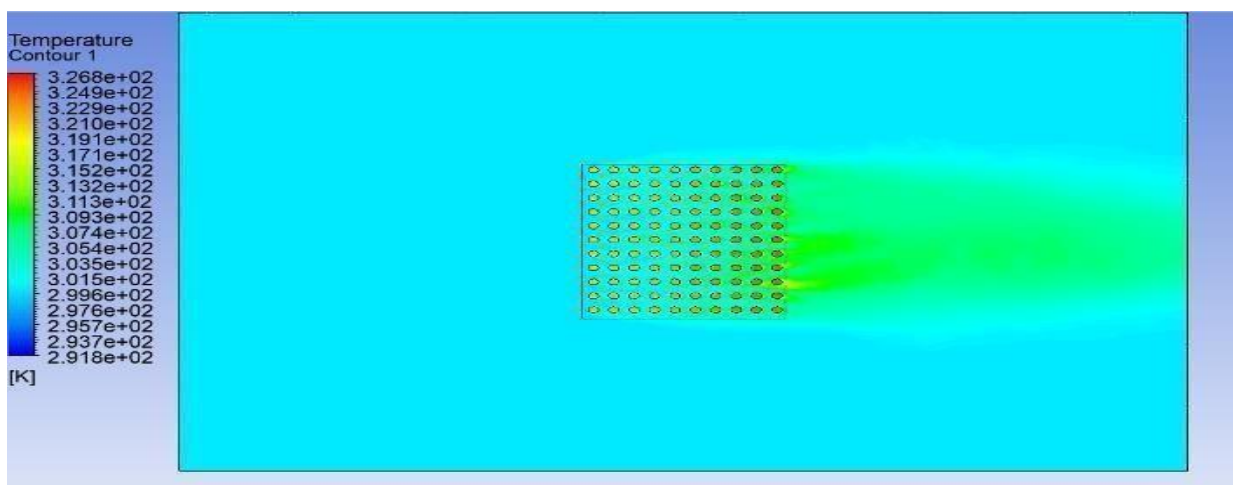


Fig 1.10: contour illustrates the lowest temperature distribution of an ellipse fin heat sink while moves velocity 12 m/s

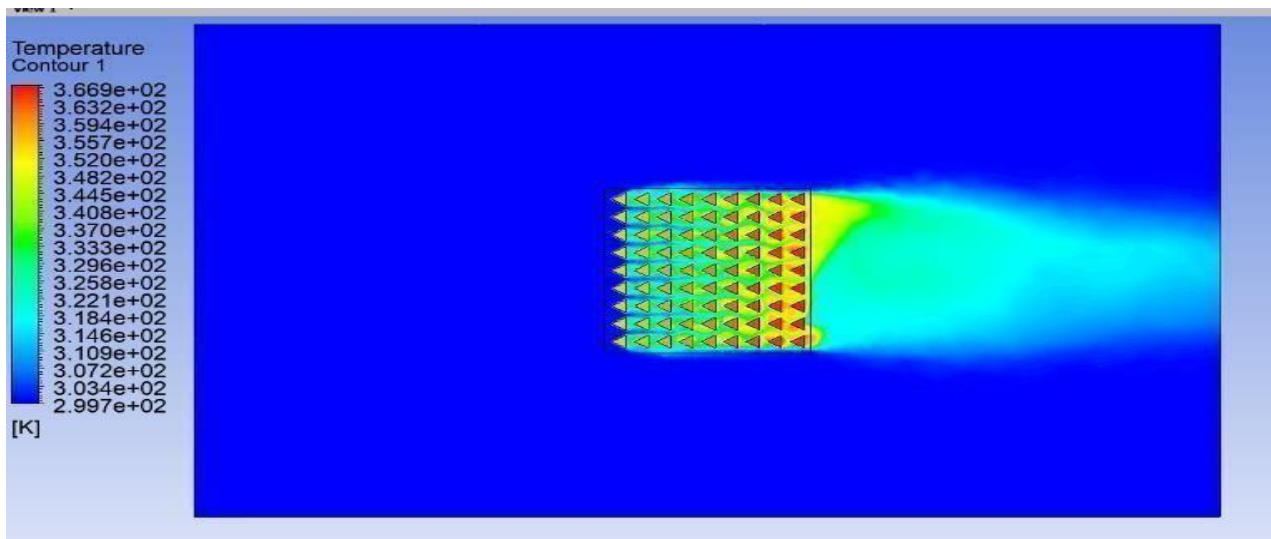


Fig 1.11: contour illustrates the lowest temperature distribution of Triangular fin heat sink while moves velocity 4 m/s

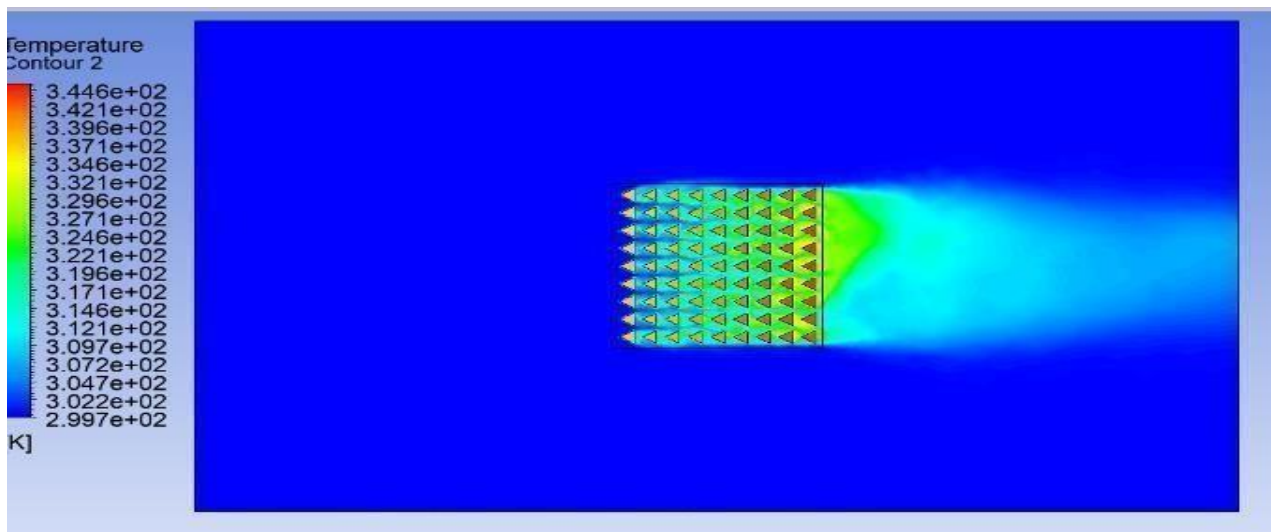


Fig 1.12: contour illustrates the lowest temperature distribution of Triangular fin heat sink while moves velocity 8 m/s

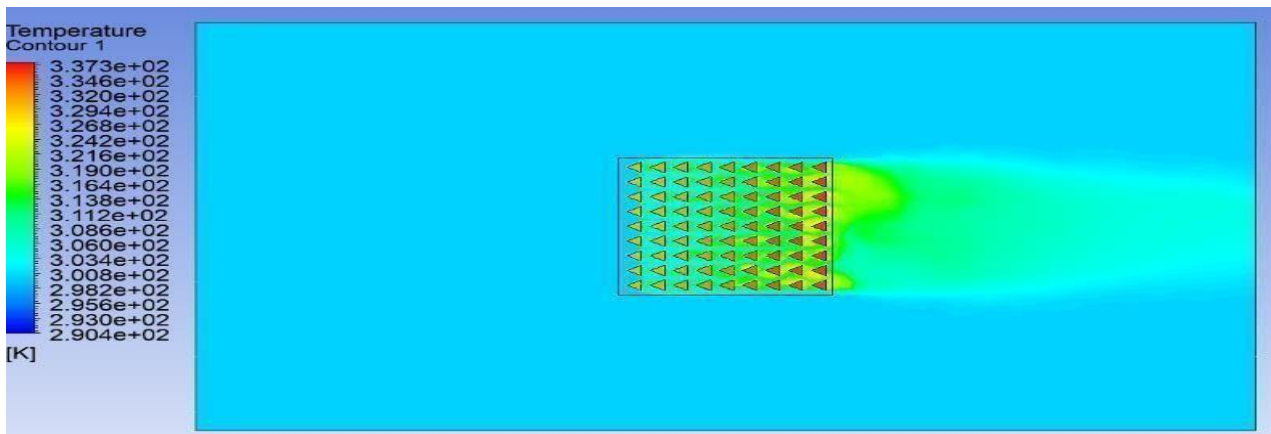


Fig 1.13: contour illustrates the lowest temperature distribution of Triangular fin heat sink while moves velocity at 12 m/s

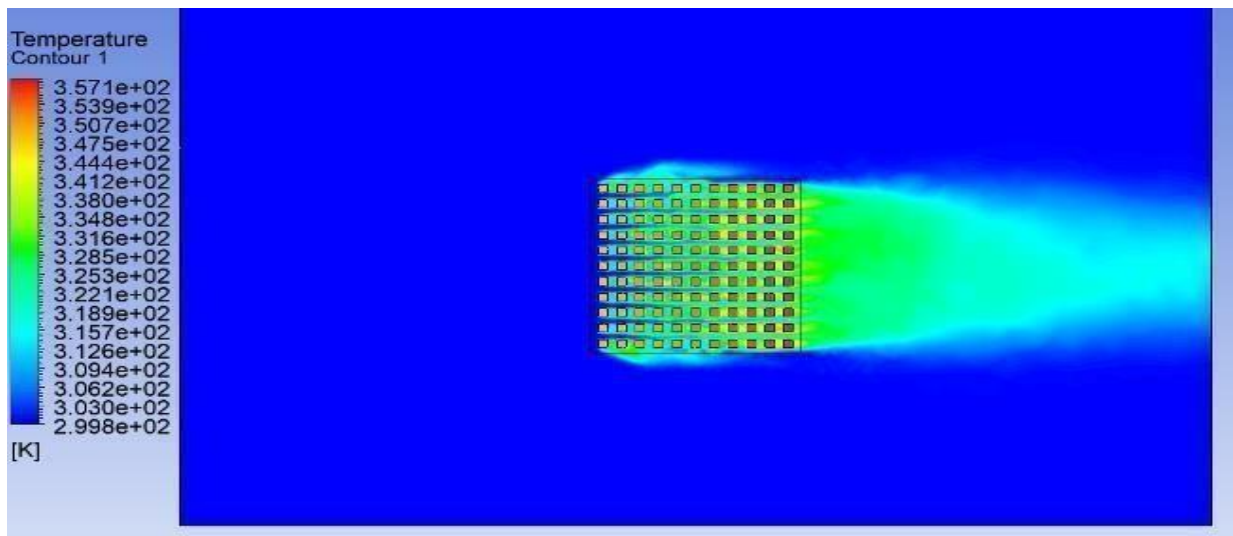


Fig 1.14: contour illustrates the lowest temperature distribution of Square fin heat sink while moves velocity 4 m/s

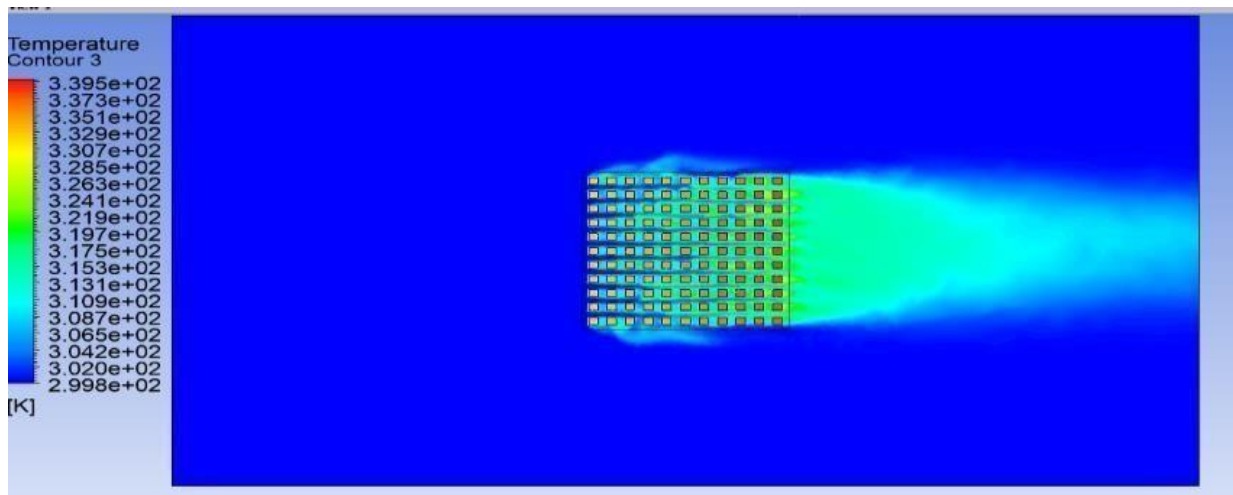


Fig 1.15: contour illustrates the lowest temperature distribution of Square fin heat sink while moves velocity 8 m/s

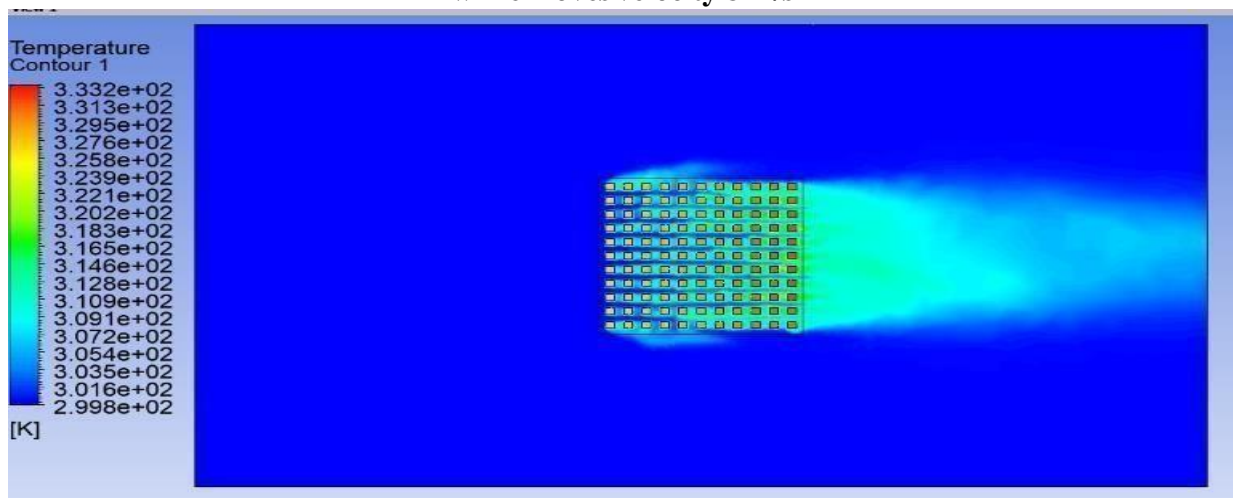


Fig 1.16: contour illustrates the lowest temperature distribution of Square fin heat sink while moves velocity 12 m/s

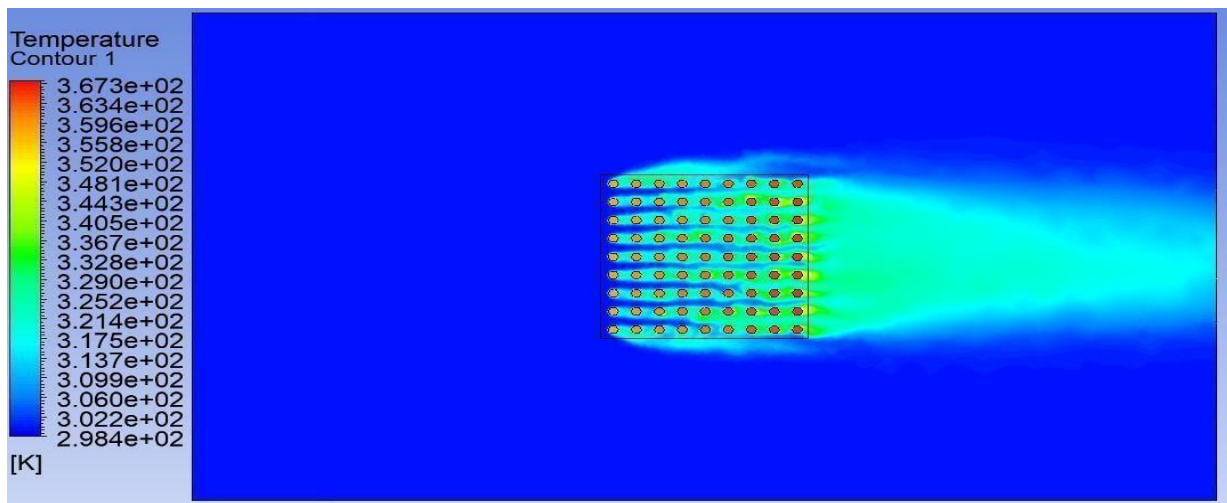


Fig 1.17: contour illustrates the lowest temperature distribution of Hexagonal fin heat sink while moves velocity at 4 m/s

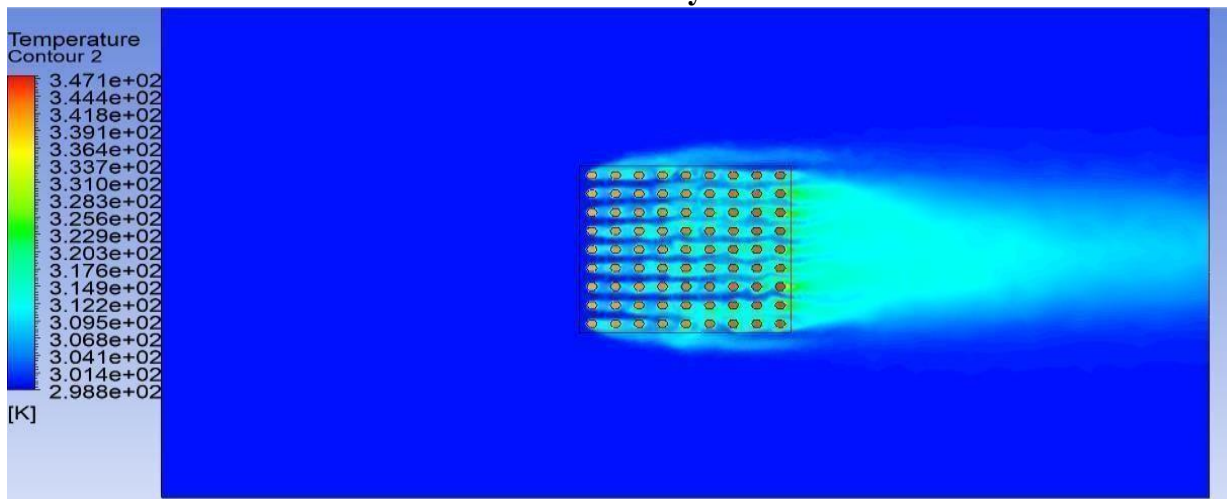


Fig 1.18: contour illustrates the lowest temperature distribution of Hexagonal fin heat sink while moves velocity at 8 m/s

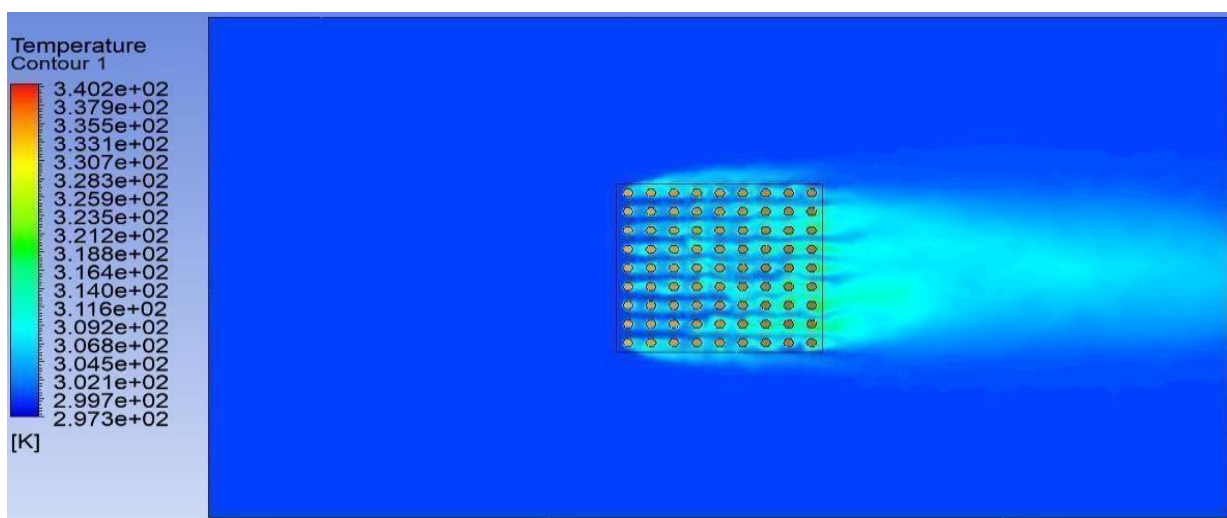


Fig 1.19: contour illustrates the lowest temperature distribution of Hexagonal fin heat sink while moves velocity at 12 m/s

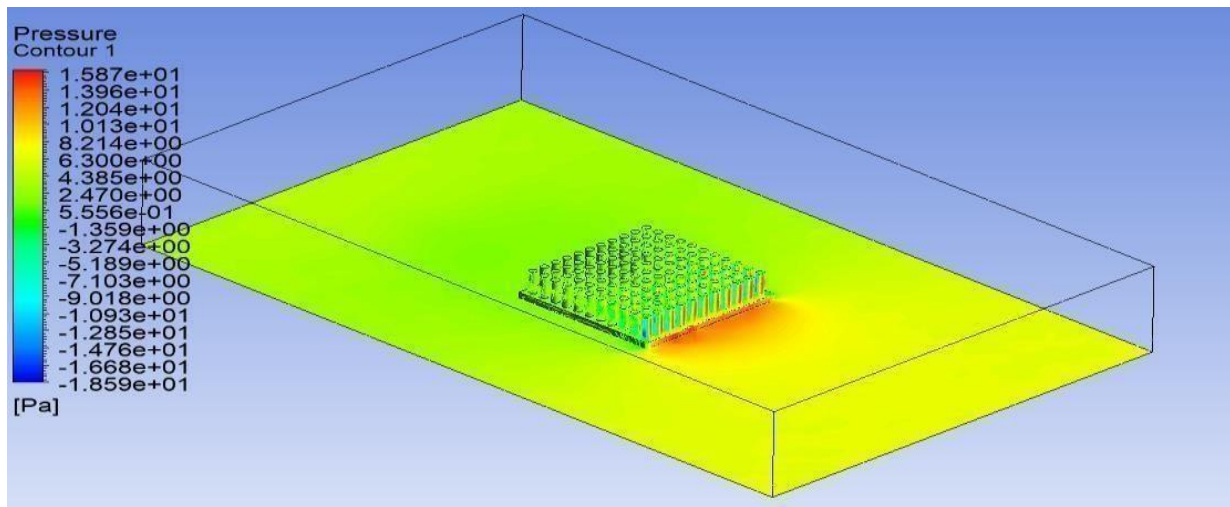


Fig 1.20: minimum pressure distribution contour for a circular pin fin heat sink at a velocity of 4m/s.

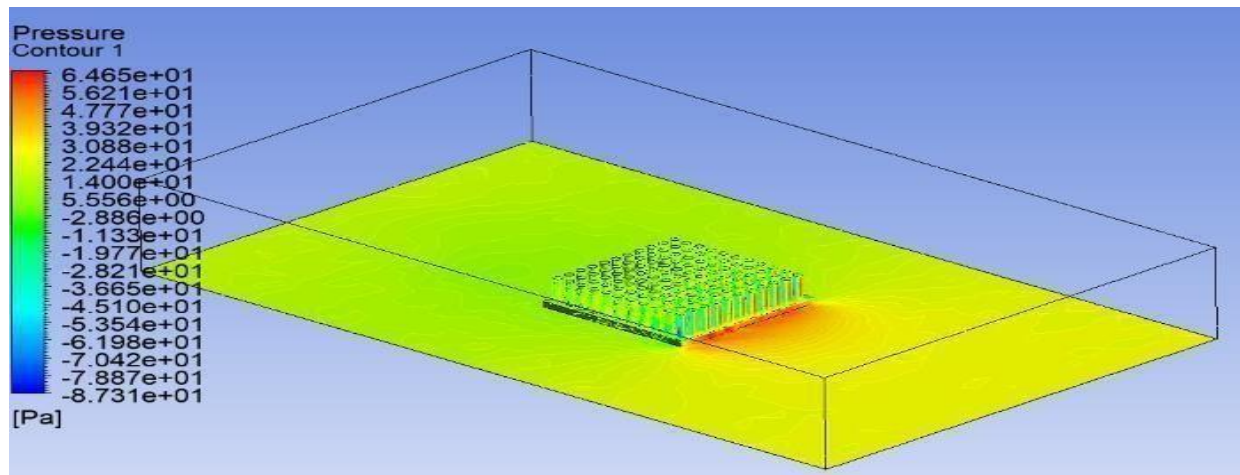


Fig 1.21: minimum pressure distribution contour for a circular pin fin heat sink at a velocity of 8m/s.

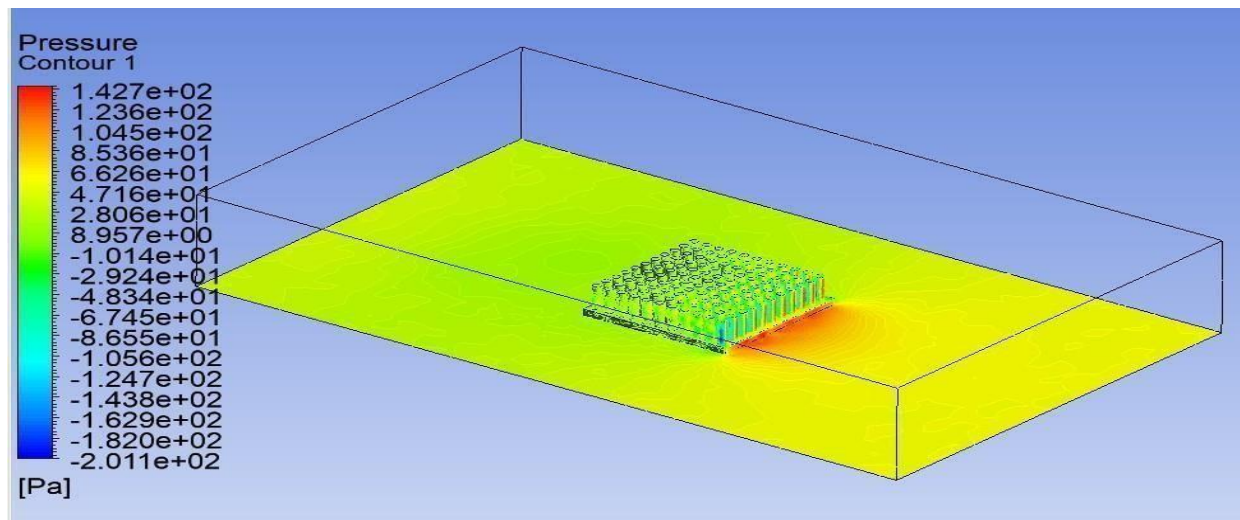


Fig 1.22: minimum pressure distribution contour for a circular pin fin heat sink at a velocity of 12m/s.

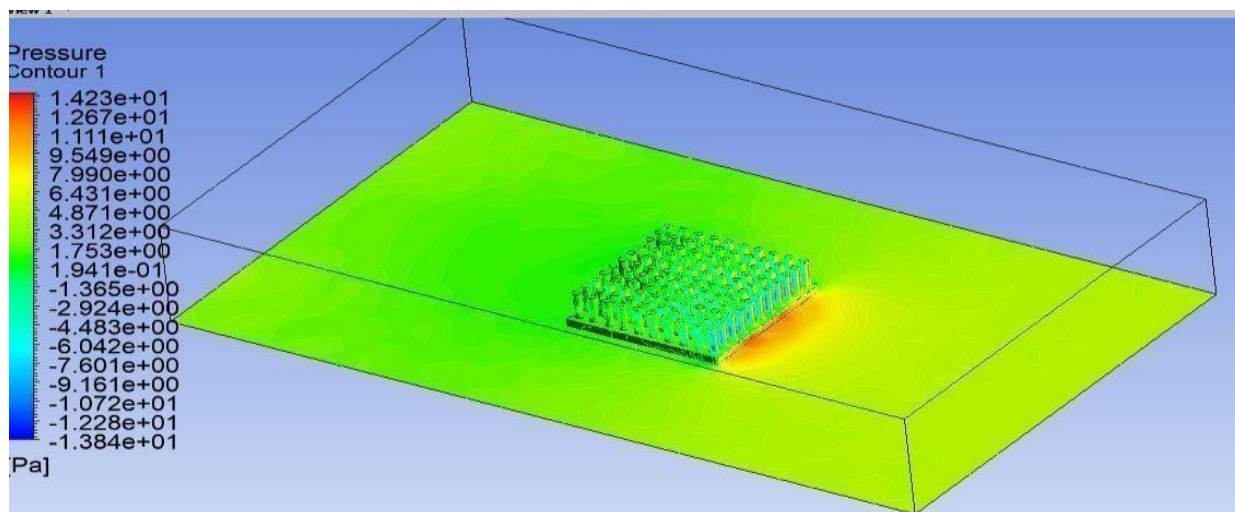


Fig 1.23: minimum pressure distribution contour for an ellipse pin fin heat sink at a velocity of 4m/s.

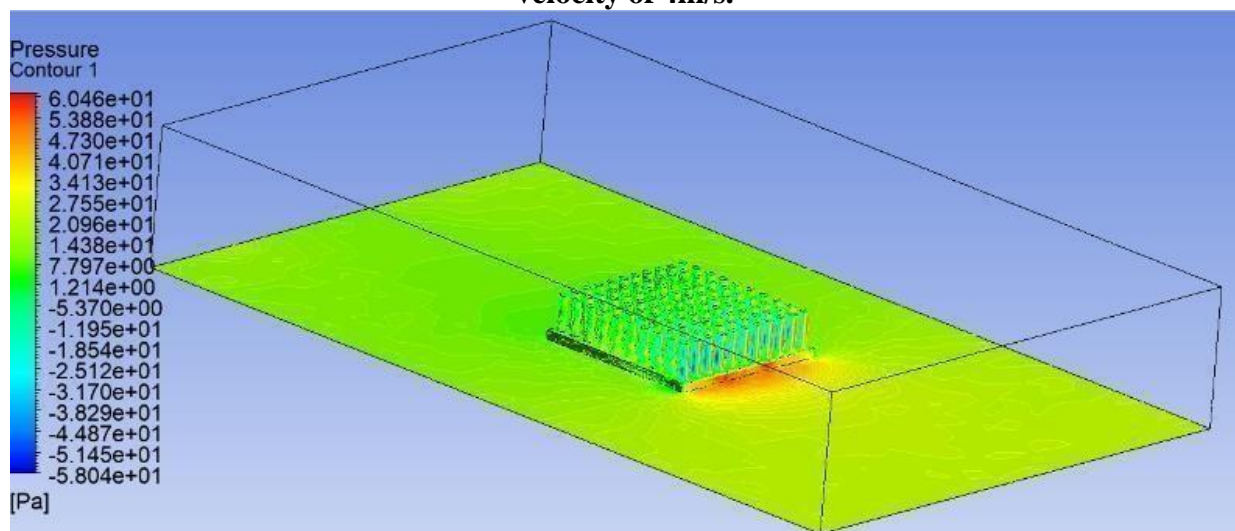


Fig 1.24: minimum pressure distribution contour for an ellipse pin fin heat sink at a velocity of 8m/s.

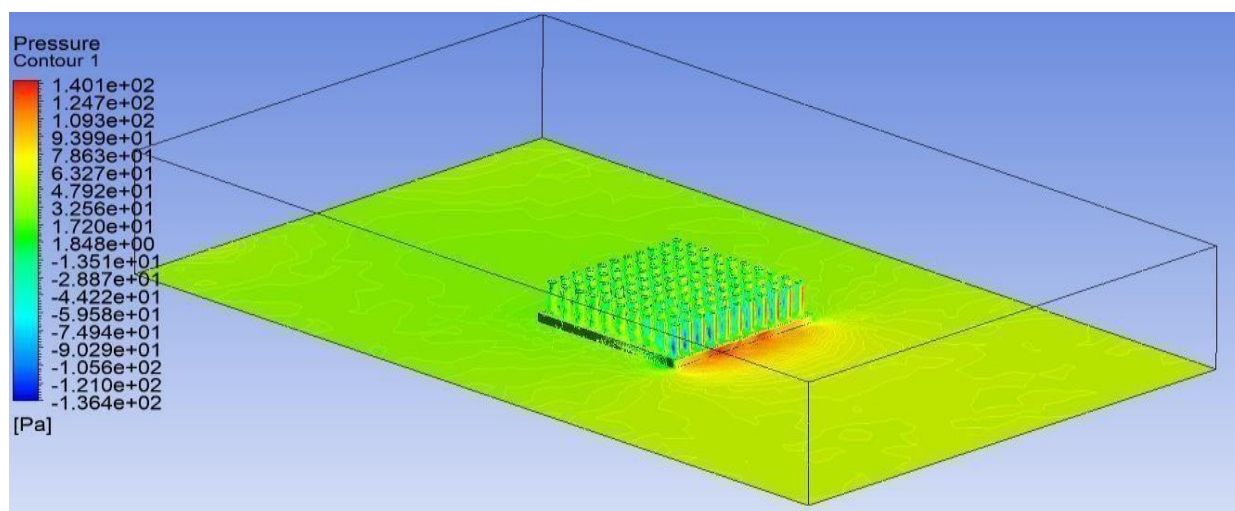


Fig 1.25: minimum pressure distribution contour for an ellipse pin fin heat sink at a velocity of 12m/s

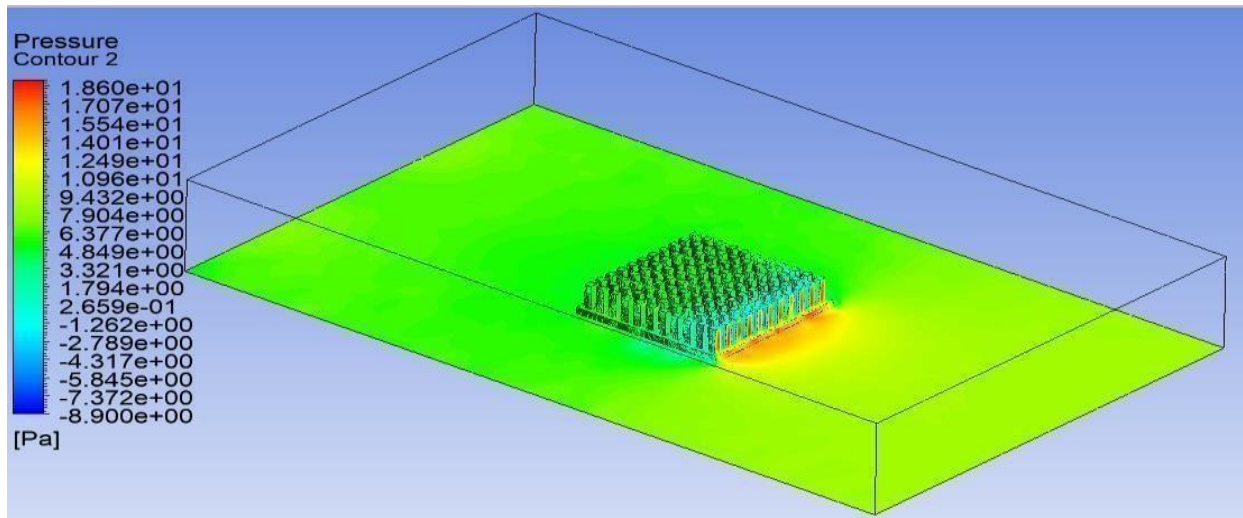


Fig 1.26: minimum pressure distribution contour for Square pin fin heat sink at a velocity of 4m/s

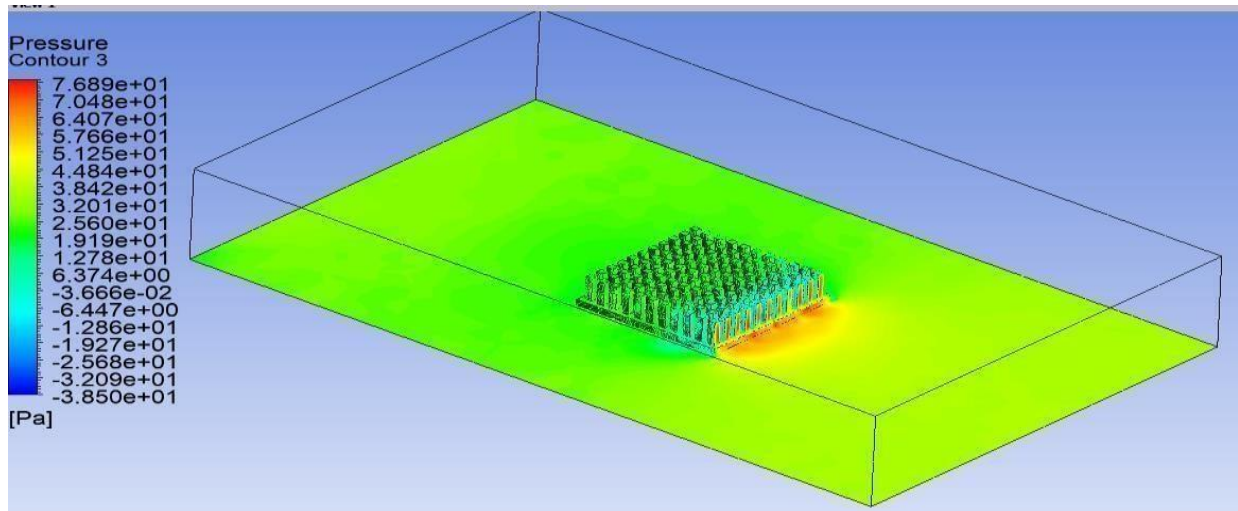


Fig 1.27: minimum pressure distribution contour for Square pin fin heat sink at a velocity of 8 m/s.

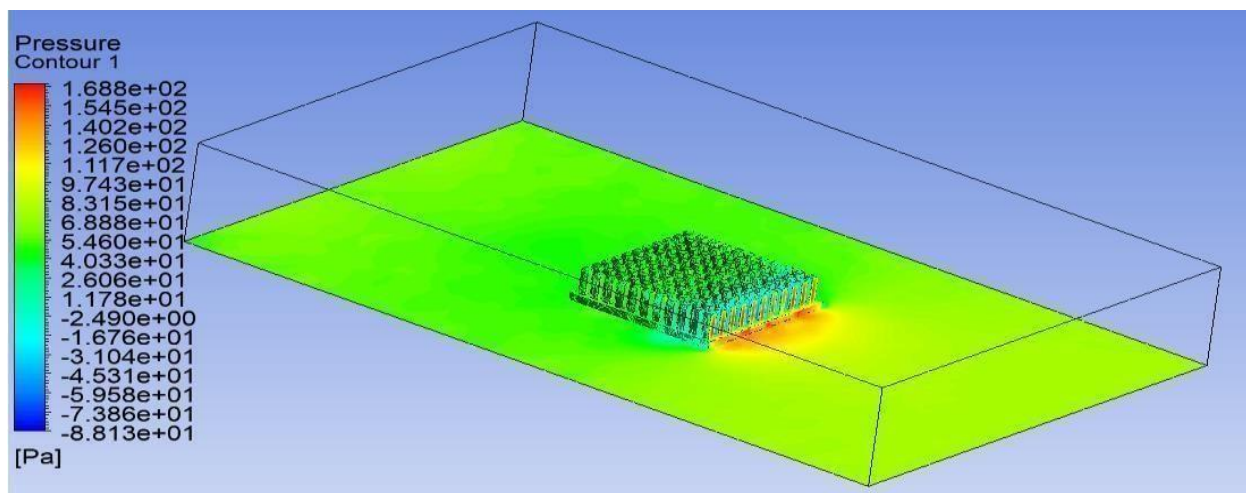


Fig 1.28: minimum pressure distribution contour for Square pin fin heat sink at a velocity of 12m/s

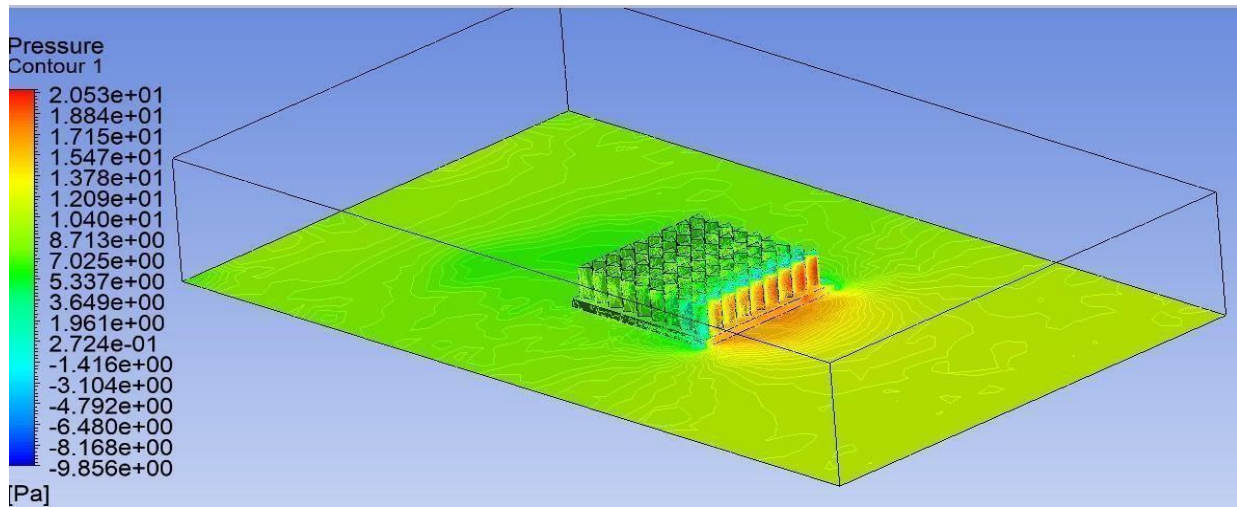


Fig 1.29: minimum distribution contour for triangular pin fin heat sink at a velocity of 4m/s

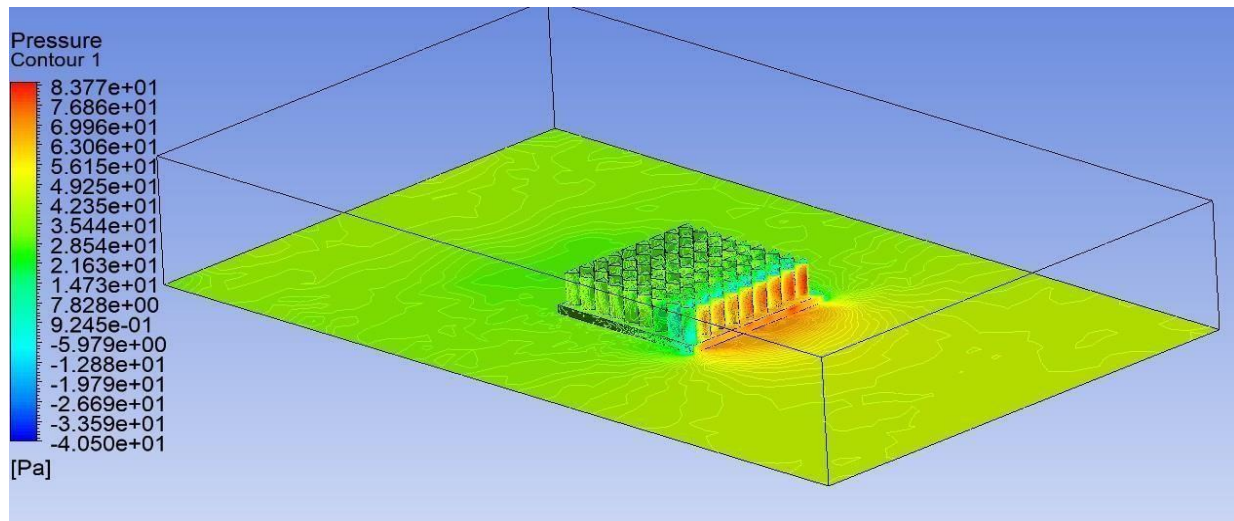


Fig.1.30: minimum distribution contour for triangular pin fin heat sink at a velocity of 8m/s

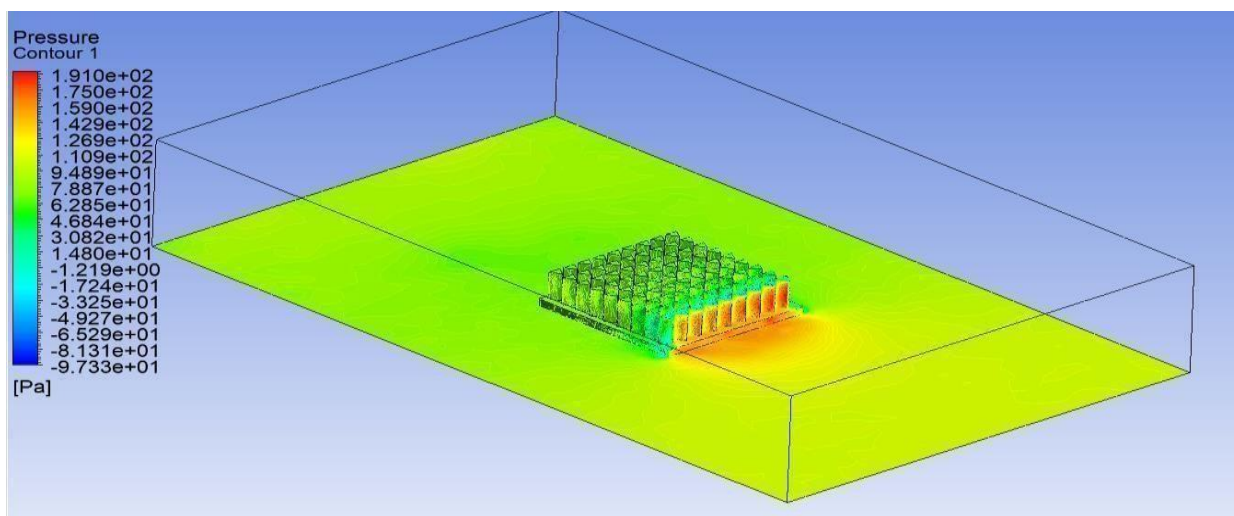


Fig 1.31: minimum distribution contour for triangular pin fin heat sink at a velocity of 12m/s

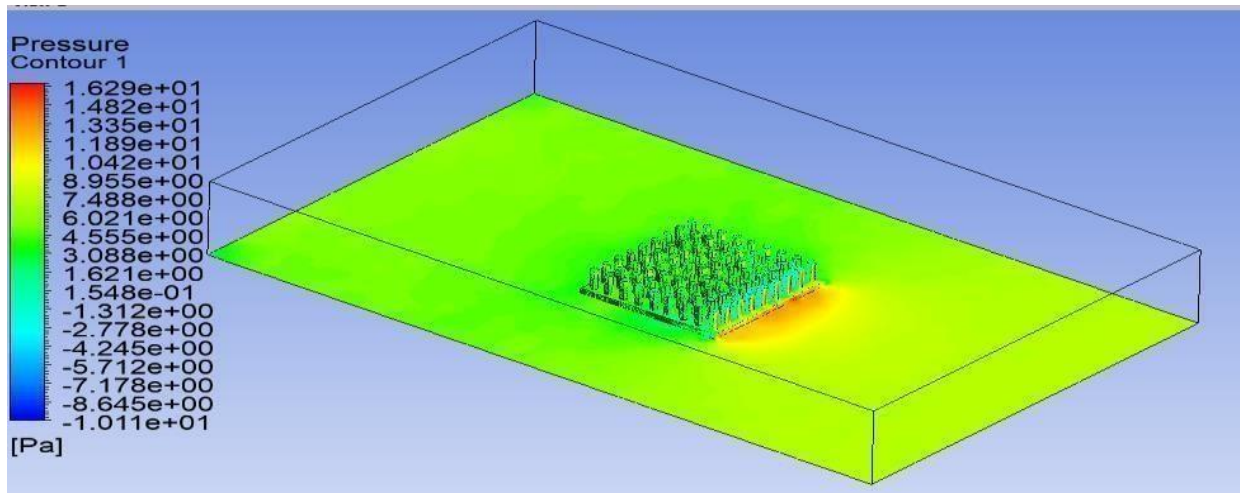


Fig 1.32: minimum distribution contour for triangular pin fin heat sink at a velocity of 4m/s.

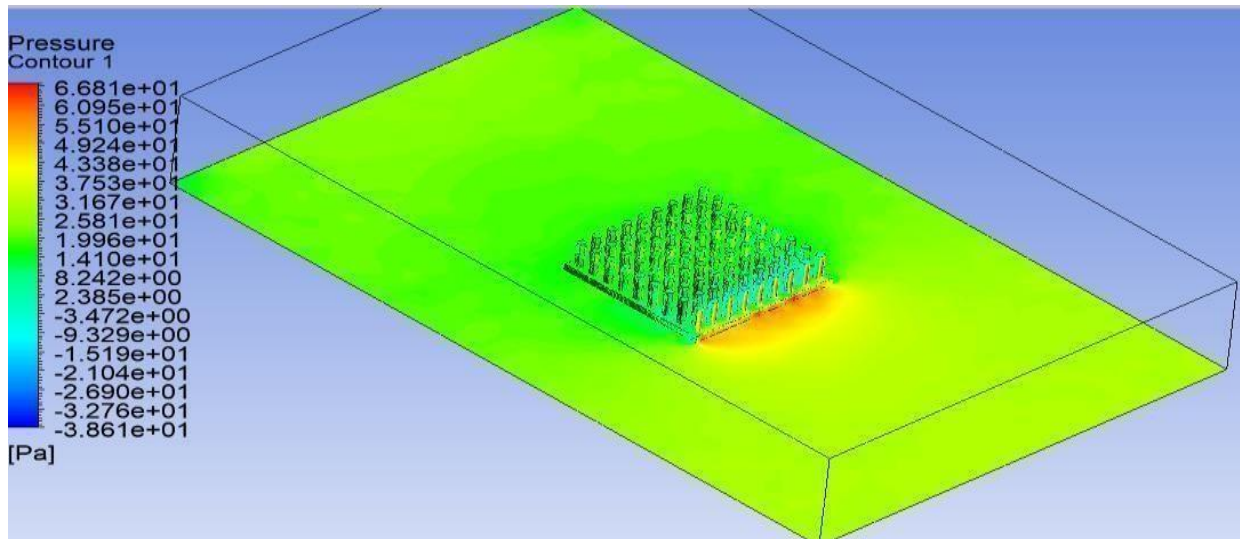


Fig 1.33: minimum distribution contour for Hexagonal pin fin heat sink at a velocity of 8m/s.

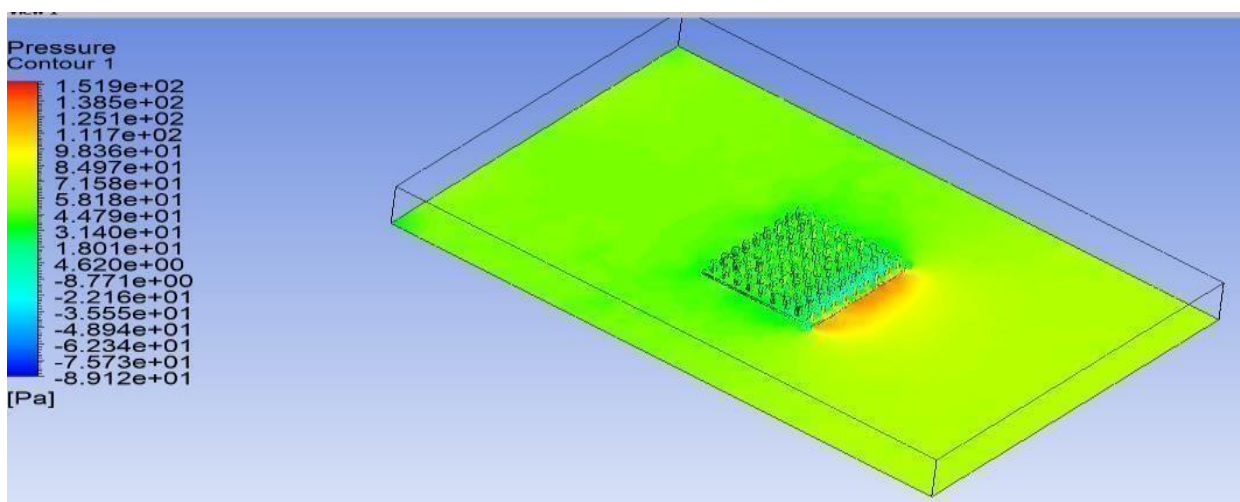


Fig 1.34: minimum distribution contour for Hexagonal pin fin heat sink at a velocity of 12m/s.

Table 1.2: shows the computation results for Circular fin profiles at 4, 8, and 12 m/s.

Circular Shape fins	Inlet velocity		
	4(m/s)	8(m/s)	12(m/s)
Thermal Resistance (K/KW)	6.422	4.33344	3.688
Pressure Drop (Pa)	7.66	33.77	76.44
heat transfer coefficient (W/m^2K)	155.7	230.17	272.72

In circular shaped fin thermal resistance decreases as per given 4m/s,8m/s,12m/s thermal resistance is 6.422k/kw, 4.33k/kw, 3.688k/kw. In case of pressure drop (pa) scenario is different for given velocities pressure drop is 4.66Pa, 33.77Pa, and 76.44Pa. Convective heat transfer coefficient is important parameter of thermal analysis of heat sink, in this Scenario heat transfer coefficient with respect given velocities it increases by 155.7w/m²K, 230.17w/m²k, 272.72w/m²k

In Square shape for given in inlet velocities we can see that thermal resistance 6.344k/kw, 3.68k/kw, 3.7k/kw, In case of pressure drop for selected velocities pressure drop is 7.64 Pa, 32.09 Pa, 71.45 Pa convective heat transfer coefficient changes as per velocities is like 157.61w/m²K, 227.17w/m²k, 271.084w/m²k. Thermal resistance is inversely proportional to given velocities, reduction in thermal resistance which is positive thing because when thermal resistance is minimum then heat dissipation is more. Pressure drop is directly proportional to increase in velocities, heat transfer coefficient is directly proportional increase in velocities. In comparison with circular and square shape fin we can see that thermal resistance of circular fin is slightly higher as compare to square shape fin

Table 1.3: shows the computation result Square fin profiles at 4, 8, and 12 m/s

Square Shape fins	Inlet velocity		
	4(m/s)	8(m/s)	12(m/s)
Thermal Resistance (K/KW)	6.344	3.68	3.7
Pressure Drop (Pa)	7.64	32.09	71.45
heat transfer coefficient (W/m^2K)	157.61	227.84	271.084

Table 1.4: shows computation result Hexagonal fin profiles at 4, 8, and 12 m/s

Hexagonal Shape fins	Inlet velocity		
	4(m/s)	8(m/s)	12(m/s)
Thermal Resistance (K/KW)	7.47	5.23	4.46
Pressure Drop (Pa)	7.33	23.43	66.93
heat transfer coefficient (W/m^2K)	133.72	191.08	223.88

Here we can see that in hexagonal shape fin for given in inlet velocities we can see that thermal resistance 7.47k/kw, 5.23k/kw, 4.46k/kw, In case of pressure drop for selected velocities pressure drop is 7.33 Pa, 23.43 Pa, 66.93 Pa. convective heat transfer coefficient changes as per velocities is like 133.72.61w/m²K, 191.08w/m²k, 223.88w/m²k

Table 1.5: shows the computation result Elliptical fin profiles at 4, 8, and 12 m/s

Elliptical Shape fins	Inlet velocity		
	4(m/s)	8(m/s)	12(m/s)
Thermal Resistance (K/KW)	5.34	3.62	2.97
Pressure Drop (Pa)	4.68	22.33	61.47
heat transfer coefficient (W/m^2K)	187.11	276.07	335.82

For analysis of Elliptical shape fin for given in inlet velocities we can see that thermal resistance 5.34k/kw, 3.62 k/kw, 2.97k/kw, in case of pressure drop for selected velocities pressure drop is 4.68Pa,22.33 Pa, 61.47Pa. convective heat transfer coefficient changes as per velocities is like 187.11w/m²K, 276.07w/m²k, 335.82/m²k In comparison with circular and square shape fin, hexagonal shape, triangular shape fin we can see that elliptical shape has advantage for more heat dissipation because thermal resistance is minimum ascompare to other shape of fins

Table 1.6: shows the computation result Triangular fin profiles at 4, 8, and 12 m/s

Triangular Shape fins	Inlet velocity		
	4(m/s)	8(m/s)	12(m/s)
Thermal Resistance (K/KW)	7.433	4.95	4.14
Pressure Drop (Pa)	10.13	34.52	80.1
heat transfer coefficient (W/m^2K)	134.52	201.79	241.28

For analysis of triangular shape fin for given in inlet velocities we can see that thermal resistance 7.433k/kw, 4.95k/kw, 4.14k/kw, in case of pressure drop for selected velocities pressure drop is 10.13 Pa,34.52 Pa, 80.1 Pa. convective heat transfer coefficient changes as per velocities is like 134.52w/m²K, 201.79w/m²k, 241.28/m²k

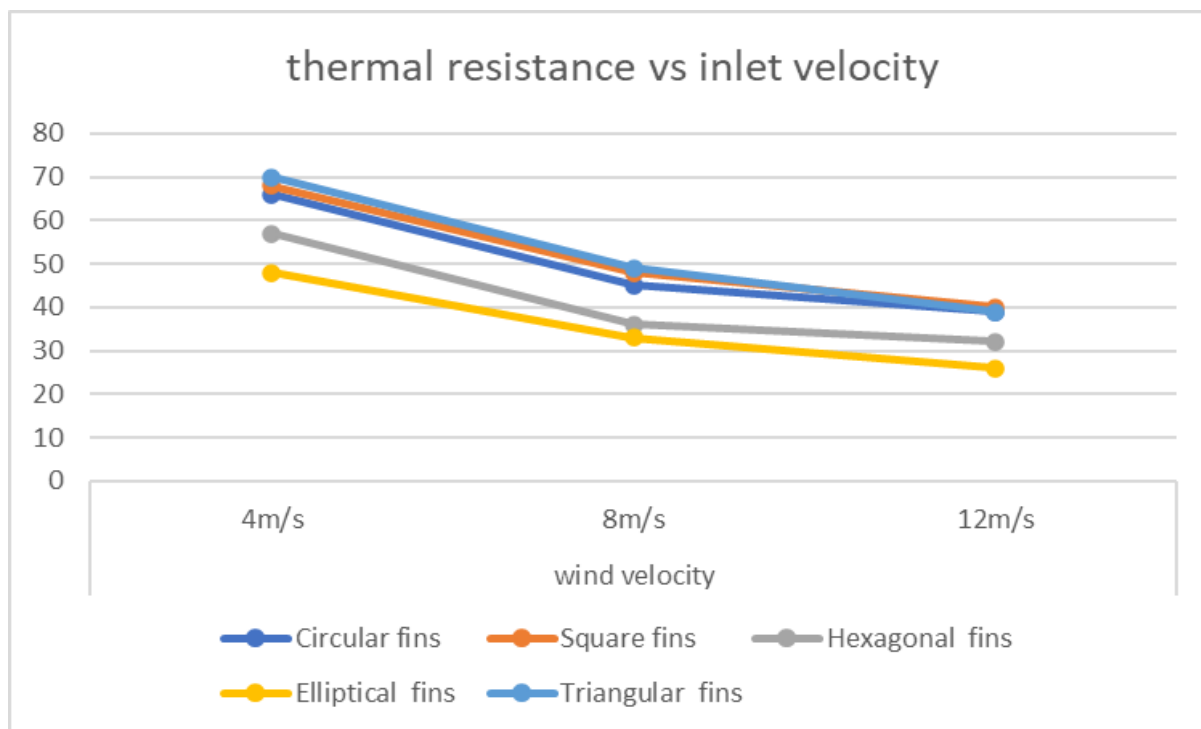


Fig 1.35: Represent a decrease in thermal resistance with an increasing inlet velocity of air of different heat sink

For various inlet air velocities, Fig1.34 shows the thermal resistance of the heat sink. Because more heat is delivered to the air as the inlet velocity rises, the thermal resistance of the heat sink reduces. Compared to 4 and 8 m/s inlet velocities, 12 m/s inlet velocity has the lowest thermal resistance. An elliptical pin fin from the heat sink has the least amount of thermal resistance for the specified inlet velocities, as can be seen.

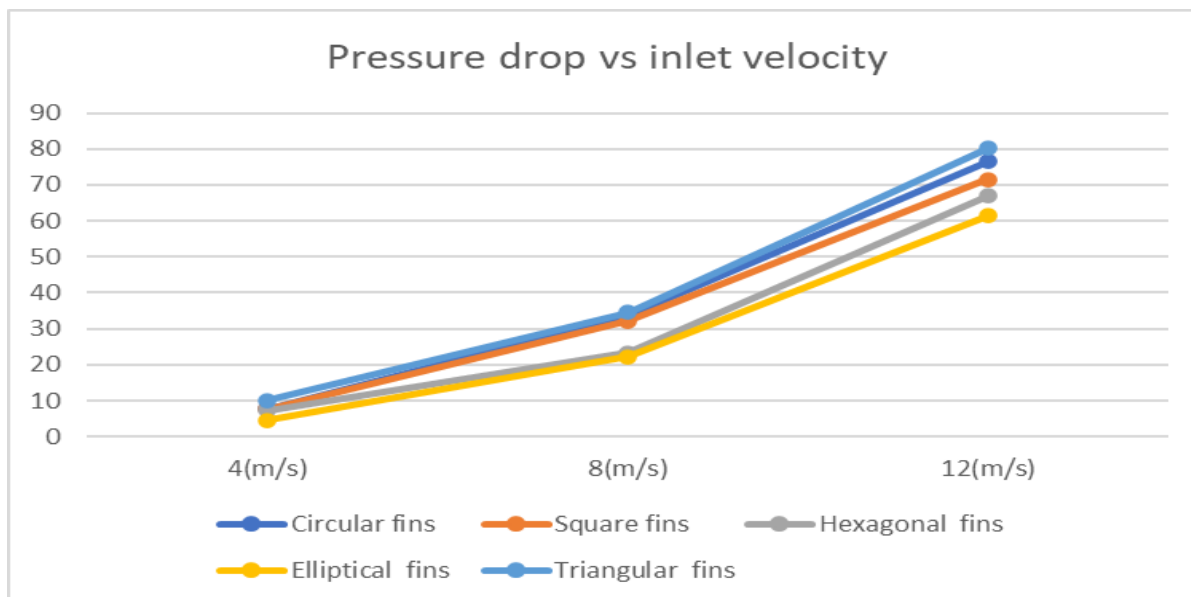


Fig 1.36: Represent the air inlet velocity and pressure drop of various heat sink profiles.

For following inlet air velocities, Fig1.35 shows the pressure drop (pa) of the heat sink. As the air inlet velocity rises, the pressure drop of the heat sink increases. Compared to 4 and 8 m/s inlet velocities, 12 m/s inlet velocity has the highest pressure drop. An elliptical pin fin from the heat sink has the minimum pressure drop for the specified inlet velocities

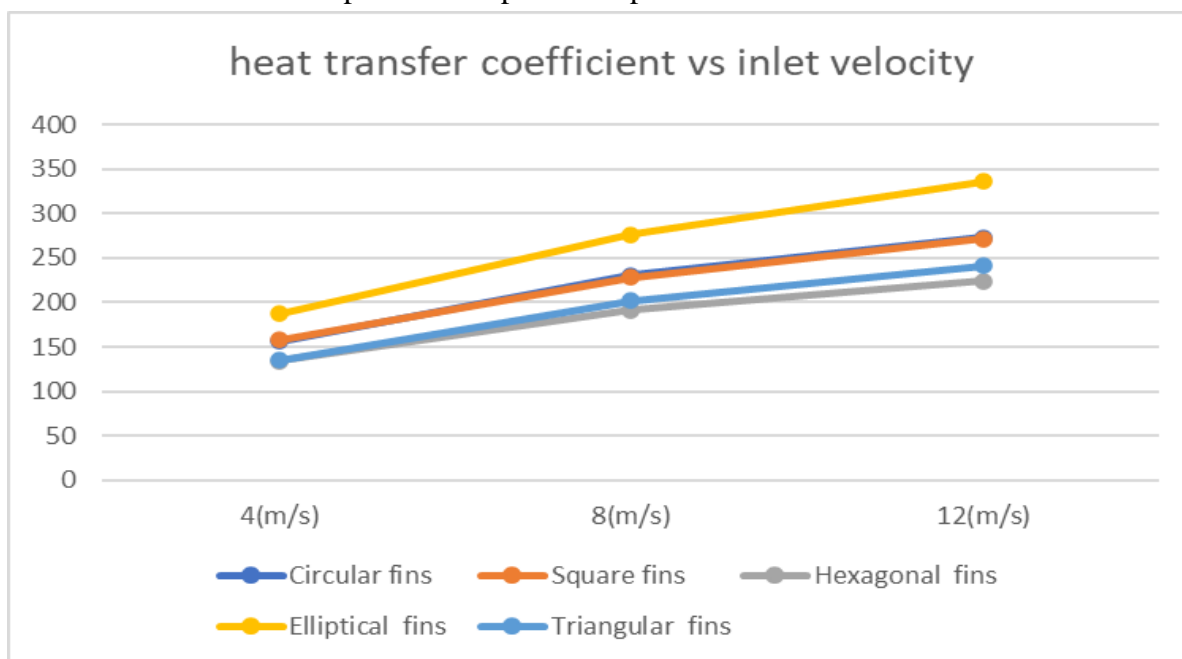


Fig 1.37: Represent the air inlet velocity and Convective heat transfer coefficient of various heat sink profiles

The convective heat transfer coefficient of the heat sink is shown in Fig1.36 for the following inlet air velocities. The convective heat transfer coefficient of the heat sink rises as the air inlet velocity rises. The greatest pressure decrease occurs at an input velocity of 12 m/s when compared to 4 and 8 m/s. The highest heat transfer coefficient for the specified intake velocities is provided by an elliptical pin fin from the heat sink.

CONCLUSION

In this study, the effectiveness of five heat sinks with differently shaped pin-fin structures was analyzed for a range of speeds, including 4, 8, and 12 m/s. This study presents the simulation and thermal analysis of different types of fin heat sinks used for electronics cooled by natural convection.

The study evaluated various fin profiles to identify the most effective heat sink designs that can enhance the rate of heat dissipation, and this can result in thermal enhancements along with reduced space requirements and material consumption, were realized. Utilizing CFD allows for improvements to heat sink designs. In the end, a new heat sink design that employs less material and performs thermally better may be produced.

Aluminum 6061 was selected as the material for the heat sink due to its lightweight nature and high thermal conductivity.

Based on the provided data on thermal resistivity, heat transfer coefficient, and pressure drop, we can come to the conclusion that the pressure drops range from a minimum of 4 Pascals to a maximum of 80.1 Pascals. Additionally, the thermal resistance values range from 2.9 inches to 7.477 inches.

According to the computational results, the elliptical pin fin with a hydraulic diameter of 4.51 mm and a fin spacing of 3.38 mm exhibits superior performance compared to the other pin fin configuration.

References

- 1) S. Ravikumar et al 2017, Experimental and Transient Thermal Analysis of Heat Sink Fin for CPUprocessor for better performance, *Frontiers in Automobile and Mechanical Engineering* 2017. 012085
- 2) Eva C. Silva, Álvaro M. Sampaio, and António J. Pontes, Evaluation of Active Heat Sinks Design under Forced Convection Effect of Geometric and Boundary Parameters, *Materials* 2021, 14, 2041
- 3) Mathias Ekpu, Raj Bhatti, N.N. Ekere and S. Mallik, Investigation of effects of heat sinks on Thermal performance of microelectronic package November 2011, (ICAST 2011) 978-1- 4673-0759-8/11
- 4) jeevaraj.s , design and simulation of heat sink for high power electronics using cfd 2013, *ijsrmissn (e)*:2321-3418
- 5) Syeda Romana, S.Shahar Banu, Md Irfan Alic, M. A. Mujeeb Iqbal, Naseemae and S.Irfan Sadaq, Thermal Analysis Of Heat Sink, *Materials Today: Proceedings* 5 (2018) 5481–5486
- 6) Haydar Kepekci, Alpay Asma, Comparative Analysis Of Heat Sink Performance Using Different Materials, *American Journal of Engineering Research (AJER)* 2020, e-ISSN: 2320-0847p-ISSN:2320-0936
- 7) Mahendra M, Salma Fathima, Mohammed Mathenulla Shariff, Altafahmed M K, and Nisar Pasha, Design and CFD Analysis of Micro-Fin Heat Sink, (*IJERT*), ISSN: 2278-0181, Vol. 9 Issue 07, July- 2020
- 8) V. Himachandra raju, ch. Srinivasa rao, steady state thermal analysis of a heat sink with Rectangular Pin fin, (*IJRASET*), ISSN: 2321-9653
- 9) R. Mohan and P. Govindarajan, Experimental and CFD analysis of heat sinks with base plate for CPU cooling, *Journal of Mechanical Science and Technology* 25 (8) (2011) 2003~2012
- 10) V Naga Raju, P. Sivakumar, K Lakshmi Narayana, A Srujan, K Mallikarjun and G Krishna, ISSN Print: 0976-6340 and ISSN Online: 0976-6359
- 11) M. Praveen Kumar and A. C. Uma Maheshwar Rao CFD Analysis on Electronic Heat Sink of Al and Cu Metals, ISSN (Online): 2581-5792
- 12) Santosh Kansal and Piyush Laad, Performance & Thermal Analysis of Heat Sink with Fins of Different Configuration Using CFD, ISSN 2229-5518
- 13) Mohammed Imran, Syed Abdul Moeed, Design and Simulation of Heat Sink for Different points Geometry with Various Heat Capacities, ISSN: 2278-0181